Journal of Applied Polymer Science

Investigation on morphology and properties of melt compounded polyoxymethylene/carbon nanotube composites

Leyu Lin,[1] Alois K. Schlarb[1,2,3]

[1]Composite Engineering CCe, University of Kaiserslautern, 67663 Kaiserslautern, Germany
[2]INM-Leibniz-Institute for New Materials, 66123 Saarbruecken, Germany
[3]Research Center OPTIMAS, University of Kaiserslautern, 67663 Kaiserslautern, Germany
Correspondence to: L. Lin (E-mail: leyu.lin@mv.uni-kl.de)

ABSTRACT: Polyoxymethylene nanocomposites containing different contents of carbon nanotubes were produced by a two-step melt compounding process using a twin-screw extruder. The dispersion quality, thermal and mechanical properties, and the creep as well as the tribological behaviors of the nanocomposites were investigated. Morphological investigations show that the masterbatch dilution process significantly improves the dispersion quality of carbon nanotubes within polyoxymethylene matrix, and as a consequence, enhanced mechanical properties and creep resistance are gained. Furthermore, to predict the long-term property based on the short-term experimental data, the time–temperature superposition principle and Findley model were used. Master curves with extended time scale are constructed using time–temperature superposition principle to horizontally shift the short-term experimental data. The simulated results confirm the reinforced creep resistance by incorporation of the carbon nanotubes into the polymer matrix even at extended long time scale. By contrast, the tribological performance of polyoxymethylene was remarkably impaired after adding carbon nanotubes. © 2015 Wiley Periodicals, Inc. J. Appl. Polym. Sci. **2015**, *132*, 42639.

KEYWORDS: carbon nanotube; extrusion; morphology; properties and characterization; thermoplastics

Received 21 April 2015; accepted 17 June 2015
DOI: 10.1002/app.42639

INTRODUCTION

Polyoxymethylene (POM) is one of the commonly used engineering thermoplastics in many industrial applications such as automotive industry, machine and plant construction, and medical technology owing to its outstanding mechanical properties, excellent dimensional stability, friction and wear behavior, and so forth, even under influence of mechanical forces and in contact with media such as chemicals and fuels. In the past decades, different nano-sized particles were used to improve the properties of polymer matrices. Among these carbon nanotubes were one of the widely used nanofillers. As carbon nanotube (CNT) was firstly discovered by Iijima in 1991,[1] they have stimulated the development of carbon nanotube filled polymer nanocomposites for a variety of applications according to their outstanding mechanical properties with low density and high thermal as well as electrical conductivity, for instance high creep resistant polymers,[2,3] electrically conducting polymers,[4–6] and structural[7] and photovoltaic applications.[8] Their diameters locate in nano-scale, whereas they are up to 10 μm long, and can be single- and multi-walled (SWCNT and MWCNT), respectively. The extremely high aspect ratio and intrinsic properties of CNTs are expected to enhance the reinforcement efficiency at lower filler loadings compared to their competitors, such as carbon black and carbon fibers. The reinforcing efficiency of carbon nanotubes has been found to be strongly dependent on the choice of polymer matrix,[9] the type of CNT,[10] and particle/matrix interphase[9,11] as well as processing methods and the corresponding parameters.[9,12] However, their tendency to agglomerate owing to van der Waals and electrostatic forces makes it challenging to generate good CNT dispersion and distribution within the polymer matrix.[13]

CNT/thermoplastic nanocomposites are usually manufactured using melt compounding process due to its simplicity and adaptability for large-scale industrial production. To gain the optimum dispersion and distribution of CNTs using melt extrusion, optimized processing parameters such as screw configuration, screw speed, melt temperature, and residence time are imperative.[14,15] It is commonly accepted that high stress is the ideal scenario for achieving better dispersion state of CNTs in the polymer matrix. Li and Shimizu[16] observed that high shear stress resulted in homogenous MWCNT dispersion in poly(styrene-*b*-butadiene-*co*-butylene-*b*-styrene) (SBBS) matrix, and as a consequence, much better mechanical properties were obtained. Villmow *et al.*[14] have reported that an increase in the

screw speed from 100 to 500 rpm can lead to better MWCNT dispersions on MWCNT-filled polycaprolactone (PCL) due to higher energy input. Similar observations were also found by Villmow *et al.*[17] on the examination of the influence of extrusion parameters on masterbatch dilution to manufacture MWCNT/poly(lactic acid) (PLA) composites using a twin-screw extruder. Therefore, optimizing the dispersion process is vital importance for producing nanocomposites with enhanced properties.

The use of carbon nanotubes reinforced polymers for tribological applications has been reported in several studies.[18,19] Higher wear resistance and lower friction coefficient were observed as incorporating carbon nanotube into polymer matrix. By contrast, Zoo *et al.* have reported that the friction coefficient slightly increased after addition of small amount CNT (e.g., less than 0.5 wt %) into ultra-high molecular weight polyethylene. In this study, the influence of masterbatch dilution process on the dispersion state of carbon nanotubes in a polyoxymethylene has been investigated. The thermal, mechanical, and creep as well as tribological properties of carbon nanotube reinforced polyoxymethylene composites as a function of filler content were examined and attempt to find the structure-property relationship of the nanocomposites.

EXPERIMENTAL

Materials and Nanocomposites Preparation

POM (ULTRAFORM® N2320 003) with a density of 1.401 g/cm^3 and CNTs reinforced POM compound (ULTRAFORM® N2320 C BK120 Q600) with a density of 1.414 g/cm^3 that contained approximately 4 vol % CNTs were supplied by BASF SE (Ludwigshafen, Germany). This compound was used as masterbatch in this work. Nanocomposites with lower filler loadings (0.5, 1, and 2 vol %) were prepared by dilution of the masterbatch containing 4 vol % CNTs. The manufacturing of the nanocompounds was performed on a co-rotating twin-screw extruder (TSK-N 030, Theysohn Extrusionstechnik GmbH, Salzgitter, Germany) with a barrel temperature of 195°C and a screw speed of 150 rpm. A screw profile with a combination of transporting, kneading, and back flow elements was used. Before extrusion, the granules were pre-dried at 80°C for 4 h. The 4 vol % CNT filled masterbatch was re-processed with the same processing conditions to produce reference composites. Injection molding of the nanocomposites was performed on an Arburg Allrounder 420 C injection molding machine (Arburg GmbH KG., Loßburg, Germany) to produce sheets with dimensions of 50 mm long, 50 mm wide, and 4 mm thick.

Microscopic Analysis

The morphology of the nanocomposites was investigated using a Nikon ECLIPSE LV100POL optical microscope (Tokyo, Japan) operated in transmission mode. Thin slices of approximately 5-μm thick were cut perpendicular to the injection molding direction on at least three different injection molded sheets at room temperature on a rotary microtome HYRAX M 25 (Carl Zeiss MicroImaging GmbH, Göttingen, Germany). The images were taken with a microcam using a 10× magnification objective lens. A minimum of 5 mm^2 micrograph area was examined for every material. Processing of the recorded images was performed with the software MATLAB R2011a corresponding to an area of about 0.6 mm^2. The area fractions of the CNT agglomerates were calculated using certain thresholds of gray level [cf. Figure 1(b,d)].

Differential Scanning Calorimetry

The thermal properties of the composites were analyzed using a differential scanning calorimetry (DSC) Q20 apparatus (TA Instruments, New Castle, DE) in aluminum pans under nitrogen atmosphere. Samples of approximately 5 mg were heated from 30 to 200°C at a heating rate of 10°C/min and kept at this temperature for three minutes to remove any thermal history and residual stress on the material. The sample was then cooled to 30°C at the same cooling rate. Second heating regime was performed similar to the first heating and these measurements were used for determination of melting temperatures and crystallinities, respectively. The degree of crystallinity of the materials was determined by means of the ratio between the measured melting enthalpy and the enthalpy of a 100% crystalline POM that is taken as 326 J/g.[20]

Static Tensile Test

Tensile properties of the nanocomposites were determined using a universal testing machine (RetroLine 10 kN, Zwick GmbH KG, Ulm, Germany) at room temperature according to DIN EN ISO 527-2/1BB (dog-bone-shaped specimens with a cross-section of 2 × 4 mm^2) on at least 10 specimens. The crosshead speed was set at 1 and 50 mm/min for the determination of tensile modulus and tensile strength, respectively.

Dynamical Mechanical Analysis

Dynamical mechanical analysis of the composites was performed on a Q800 dynamical mechanical analysis (DMA) (TA Instruments, New Castle, DE) with single cantilever clamp at a vibration frequency of 1 Hz and amplitude of 10 μm. The temperature scan rate was set at 2°C/min from 30 to 160°C and sample dimensions were typically 17.6 mm long, 6 mm wide, and 4 mm thick.

Short-Term Creep Test

Short-term creep tests were performed on the above-mentioned DMA apparatus in single cantilever mode at different temperatures. The creep compliance was determined as a function of time (t_{creep} = 30 min) under a constant applied stress of 2 MPa, which was derived from the experimental calibration of the linear viscoelastic region, to avoid misinterpretation of creep experiments. The temperature dependence of the creep response of various materials was studied in the range from 40 to 140°C. Isothermal tests were run on the same specimen as used for DMA analysis in the above temperature range by increasing the temperature stepwise by 10°C and equilibrating the specimen at each temperature for 20 min.

Tribological Test

The tribological tests were performed using a block-on-ring apparatus with specimens having a dimension of 4 × 4 × 10 mm^3, which were directly milled from injection-molded sheets. The counterbody is a 100Cr6 steel ring with a diameter of 60 mm and a mean roughness $R_a \approx 0.2$ μm. Before the tests, the testing pins were "pre-worn" with a grinding paper (P240) to an arc outline for fitting well the configuration of the

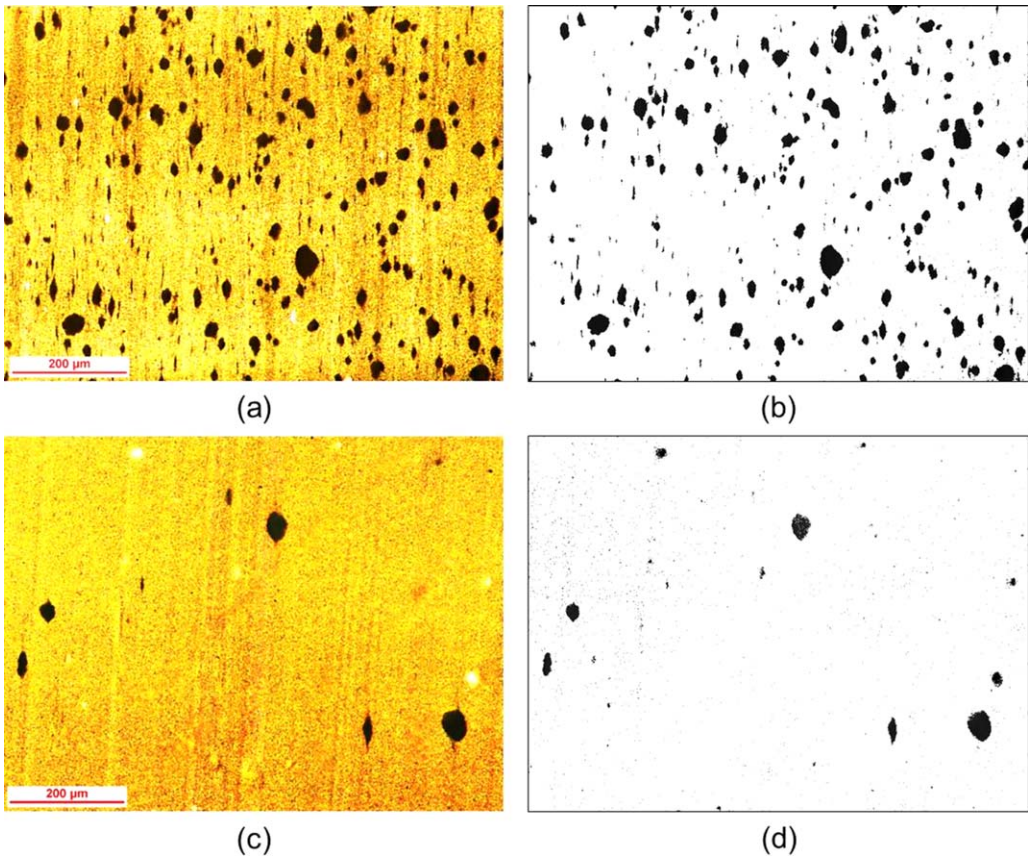

Figure 1. Representative optical micrographs of (a) and (b) masterbatch before and after image processing; (c) and (d) POM filled with 4 vol % CNT before and after image processing. [Color figure can be viewed in the online issue, which is available at wileyonlinelibrary.com.]

counterbody to reduce the running-in process. During the test, the friction force was measured and recorded into a computer dynamically. The ratio between the friction force and normal load equals the friction coefficient. For each test, the friction coefficient refers to the mean value of the data recorded after running-in process. All the tests in this work were conducted for 24 h under dry sliding condition at room temperature. The apparent pressure and sliding velocity were 1 MPa and 1 m/s, respectively. The specimen's mass loss after experiments, Δm, was measured and the specific wear rate w_s of the material was calculated using following equation:

$$w_s = \frac{\Delta m}{\rho \cdot F \cdot L}, \quad (1)$$

where ρ is the specimen density, F is the normal load applied on the specimen during the testing, and L is the total sliding distance. At least three repetitive tests were executed for calculating the mean friction coefficient and specific wear rate.

RESULTS AND DISCUSSION

Effect of Processing Variation on the Morphology of Nanocomposites

A suitable dispersion and distribution of carbon nanotubes inside the polymer matrix is a key challenge for successful industrial applications of CNT/polymer nanocomposites. The particle distribution and dispersion in the matrix is a complicated mechanism involving the wetting of agglomerates by polymer melt, infiltration of matrix into the agglomerates, and subsequently the dispersion of agglomerates. The final dispersion quality is determined by the nature and type of the matrix material and CNTs, and also the processing histories.[21] Figure 1(a,c) show the dispersion state of masterbatch and masterbatch after re-processing. The agglomerate area and count of the masterbatch with 4 vol % CNT decrease significantly when re-processing the masterbatch. The agglomerate area reduces from $8.87 \pm 3.40\%$ to $1.90 \pm 1.48\%$. The decrease in agglomerate area and count attributes to the second extrusion step which benefits the individualization of the CNTs and the de-agglomeration of the large agglomerates due to high shear stress.

The authors resorted to a morphological analysis on a scanning electron microscopy (SEM) to evaluate the dispersion state at high magnification. The morphology of the nanocomposites observed by SEM in Figure 2(a,b) shows similar results in the qualities of dispersion. As mentioned above, the composites produced by masterbatch dilution and re-processing of masterbatch [Figure 2(a)] show better dispersion quality than the masterbatch [Figure 2(b)]. The individualized CNTs can be clearly observed. In the case of the masterbatch, it is clearly obvious that large agglomerates exist in the composite.

DSC Analysis

The effect of the carbon nanotubes addition on the melting and crystallization behavior of the POM matrix was evaluated by

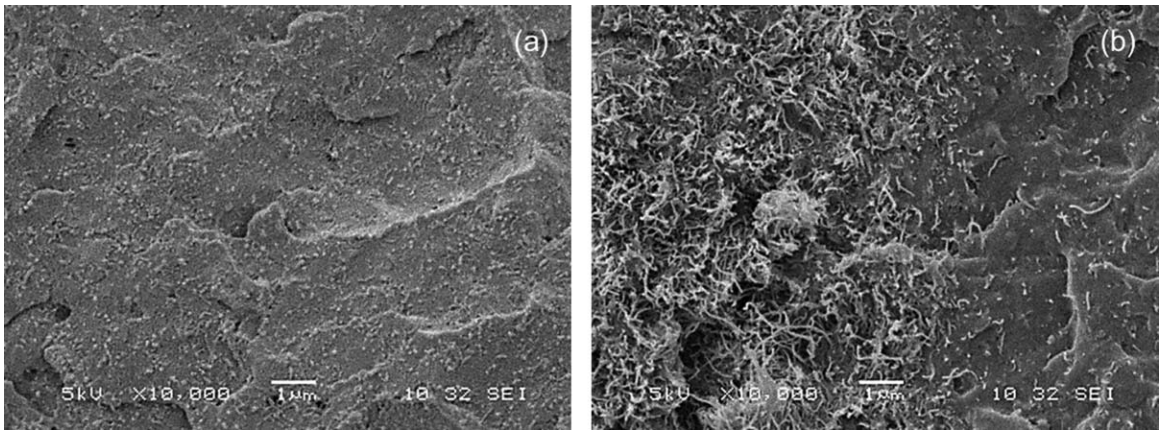

Figure 2. Representative SEM microphotographs of POM with 4 vol % CNT: (a) re-processing of masterbatch and (b) Masterbatch.

means of DSC analysis, as is shown in Figure 3. The results obtained after eliminating the entire thermal and stress histories are shown in Table I. As it can be seen, the addition of carbon nanotubes into POM does not significantly affect the melting temperature of POM matrix, the melting temperature between POM and its nanocomposites has only mirror difference (maximum 2.5°C). The cooling traces reveal that there is an exothermal peek for each sample, being attributed to POM crystallization. The crystalline peak temperatures of POM in the composites are slightly increased with a maximum value of 3°C. The crystallinity of the materials is calculated using the following equation:

$$X_c = \frac{\Delta H_m}{w_p \cdot \Delta H_c}, \quad (2)$$

where X_c is the degree of crystallinity, ΔH_m is the obtained melt enthalpy from DSC testing, w_p is the weight fraction of POM in the composites, and ΔH_c is the theoretical 100% crystallized POM, taken as 326 J/g. The results show that the addition of CNTs has insignificant influence on the crystallinity of POM matrix. A slight increase in the crystallinity up to 3.2% is observed. These observations from the DSC measurements indicate the fact that the carbon nanotubes act as nucleation sites in the composites to promote the crystallization behavior of polymer and thereby increase crystallization temperature and crystallinity. However, the increase is not pronounced, which is in good agreement with previous studies.[20,22]

Static Tensile Properties of Nanocomposites

Figure 4(a) shows the representative stress–strain curves of unreinforced POM and POM filled with 1 and 4 vol % carbon nanotubes. All the studied materials present a linear elastic behavior at the beginning of tensile tests. The mean Young's modulus, tensile strength, and strain at break of different materials are present, respectively, in Figure 4(b–d). As is clearly seen, the addition of nano-sized fillers increases the Young's modulus but decreases the strain at break of unfilled POM. The incorporation of carbon nanotubes imparts the high stiffness of the fillers to the polymer matrix [Figure 4(b)]. The elastic deformation transfer occurring in the polymer/filler interfaces accounts for the increased stiffness.[23] Increasing content of carbon nanotubes from 0.5 to 4 vol % in the studied range leads to increasing tensile modulus of POM as a result of increased interfacial area between nanofillers and polymer matrix. However, the incorporation of carbon nanotubes does not result in a pronounced improvement in the tensile strength of POM [Figure 4(c)]. The maximum improvement is found at a filler loading of 4 vol %, which is about 4% higher than the tensile

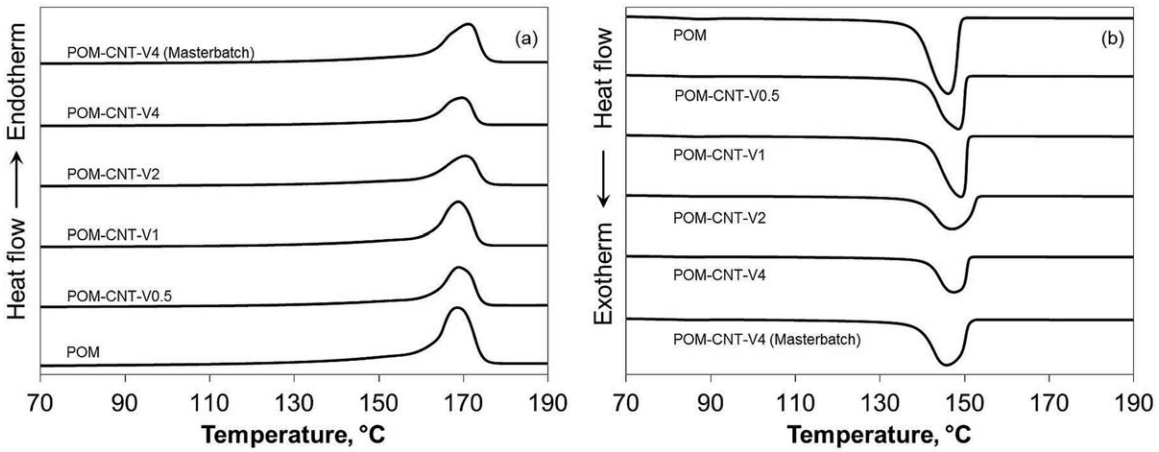

Figure 3. DSC thermograms of POM and its nanocomposites: (a) the heating curves and (b) the cooling curves.

Table I. Effect of Carbon Nanotube on the Thermal Behaviors of Polyoxymethylene

Designation	Melting temperature T_m (°C)	Crystalline temperature T_c (peak) (%)	Crystallinity X_c
POM	168.6	146.1	55.0
POM-CNT-V0.5	168.9	148.5	56.0
POM-CNT-V1	168.8	149.1	56.3
POM-CNT-V2	170.4	147.1	57.8
POM-CNT-V4	169.7	147.2	58.2
POM-CNT-V4 (Masterbatch)	171.1	145.8	56.3

strength of pure POM. By contrast, the nano-filler significantly decreases the ductility of the matrix. As seen in Figure 4(d), a sharp drop of strain at break is noticed when 0.5 vol % CNT is incorporated into the matrix. Further increase in CNT content results in a slight decrease in the ductility of the composite.

Concerning the tensile modulus and tensile strength of the masterbatch [the single point in Figure 4(b–d)], it is interesting to note that the tensile properties of the masterbatch are lower than the corresponding values of nanocomposites with the same filler loading which was produced by re-extrusion of the masterbatch. In particular, the tensile strength of the masterbatch is even slightly lower than that of virgin POM. This interesting observation can be attributed to the high amount and size of the CNT agglomerates which impair the load bearing capacity of the composites.

Dynamic Mechanical Analysis

The influence of the filler loadings on the α-transition temperature of virgin POM, which is usually attributed to the intra-chain molecular motions of long molecular segments, can be determined using DMA measurements. Here, the transition value is the temperature corresponding to the instance of maximum value of loss modulus (G'') and temperature at maximum tan delta (tan δ) inflexion.

From the DMA results, which are shown in Figure 5, it can be seen that the α-transition of POM matrix stands at 100 and 120°C obtained from loss modulus and loss factor tan δ, respectively. The incorporation of 0.5 vol % CNT into POM matrix results in respective heightening of the transition value by 2.5 and 2.9°C, which is principally a result of the filler addition resulting in an interface between the filler and matrix. Further increase in the CNT content up to 4 vol % slightly impairs the transition temperature; however, it is still higher than the corresponding temperature of virgin POM. The addition of the filler into the polymer matrix obstructs the molecular mobility of the polymer in close vicinity to the filler contributing to the

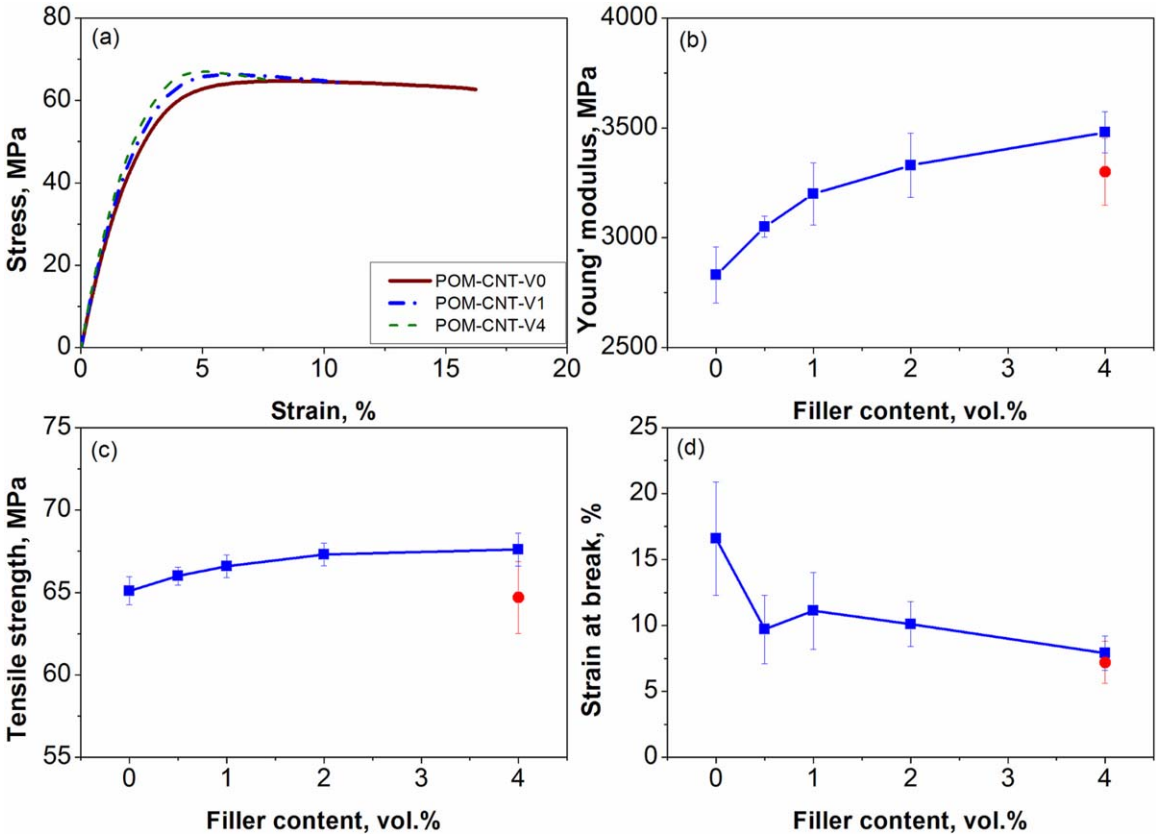

Figure 4. Tensile properties of POM and its nanocomposites as a function of filler loading: (a) representative stress–strain curve of different materials; (b) tensile modulus; (c) tensile strength; and (d) strain at break. [Color figure can be viewed in the online issue, which is available at wileyonlinelibrary.com.]

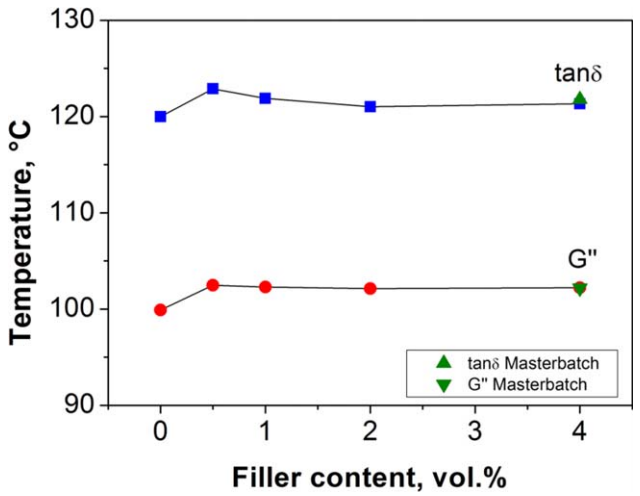

Figure 5. Observation of α-transition temperature by DMA measurements. [Color figure can be viewed in the online issue, which is available at wileyonlinelibrary.com.]

increase in α-transition temperature. The transition temperature of the intermediate layer is determined by the layer thickness and it reduces with approaching distance to the bulk polymer.[21] If the filler concentration is high, the filler–filler interaction dominates resulting in a reduction of intermediate layer owing to their overlapping. This could be a reason for the decreasing transition temperature.

Considering the α-transition temperature of the masterbatch and that of the re-processed masterbatch, no difference in the α-transition values is observed, which indicates the fact that, here, the α-transition of the POM matrix is independent on the morphology of composites (quality of filler dispersion) and the enhanced processing history.

As is well known, the decrease in the storage modulus (G') of the materials with increasing temperature is a result of the cooperative motion of polymer chains causing energy dissipation. Similar result was also observed for our nanocomposite system. The storage modulus of the nanocomposites measured by DMA is shown in Figure 6. As is shown, the incorporation of carbon nanotubes into POM led to an increase in the storage modulus in the testing range. The increase of the modulus with CNT additions is attributed primarily to the inherently higher stiffness of the filler. Increasing addition of CNT resulted in higher modulus. The composite containing 4 vol % CNT exhibited a modulus of 2315 MPa at 40°C that is about 270 MPa higher than the matrix modulus. It is also interesting to note that the modulus of the re-processed masterbatch was slightly higher than that of masterbatch. These observations point out the fact that the filler content does not alone suffice for enhancing the stiffness of the composites, but the morphology of the composites also affects the composite stiffness.

Short-Term Creep Test

The creep response evaluated from the simultaneous time and temperature dependence of the nanocomposites with different filler loadings is shown in Figure 7(a–c). It can be clearly seen that increasing temperature results in impairment of the creep resistance for all the materials studied, which can be attributed to the temperature-activated softening of the polymer matrix as a result of reduction of stiffness of the entangled network of polymer chains. Moreover, it is visible that the incorporation of nano-sized fillers causes a large reduction of the magnitude of creep compliance which indicates a pronounced improvement of creep resistance for a given temperature, as is shown in Figure 7(d), which may be the result of the restriction of the segmental mobility of the polymer chains as the nanoparticles were added into polymer matrix. However, the creep behavior is not noticeably affected by the CNT content, an increase in CNT content leads to a slight improvement in the creep resistance.

The viscoelastic behaviors of various polymers could be accurately described over a wide time scale in terms of creep strain or creep compliance using an empirical power equation known as Findley power law.[24]

Creep strain:

$$\varepsilon_F = \varepsilon_{F0} + \varepsilon_{F1} t^n, \tag{3}$$

or creep compliance:

$$J_F = J_{F0} + J_{F1} t^n, \tag{4}$$

where ε_{F0} and J_{F0} are the time-independent strain and compliance, respectively; ε_{F1} and J_{F1} are the coefficients of time-dependent terms which can be affected by stress and environmental conditions including temperature and moisture, and so forth, and n is the time exponent which is not sensitive to stress. Figure 7(d) shows the simulated curves using Findley power law, which are drawn in solid lines. It could be clearly seen that the modeling results showed a satisfactory agreement with the experimental data for each material. The values of the related parameters for matrix and nanocomposites are summarized in Table II. Both the instantaneous initial creep compliance and the time-dependent creep compliance showed obvious growth with increasing temperature for each material. In addition, it is apparent that the time-dependent creep compliance J_{F1} of the Findley power low reduced by the incorporation of

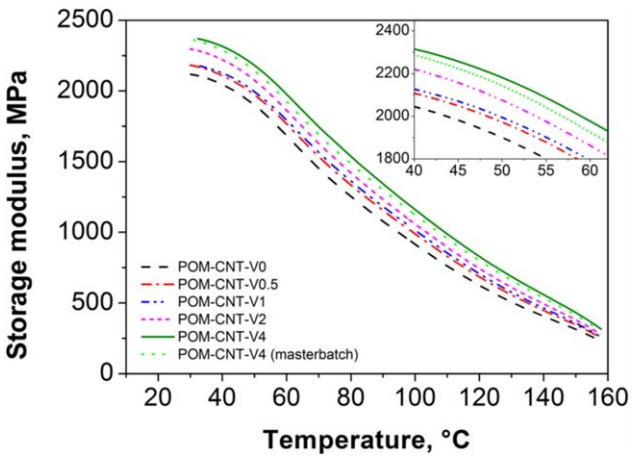

Figure 6. Variation of storage modulus as a function of filler loading. [Color figure can be viewed in the online issue, which is available at wileyonlinelibrary.com.]

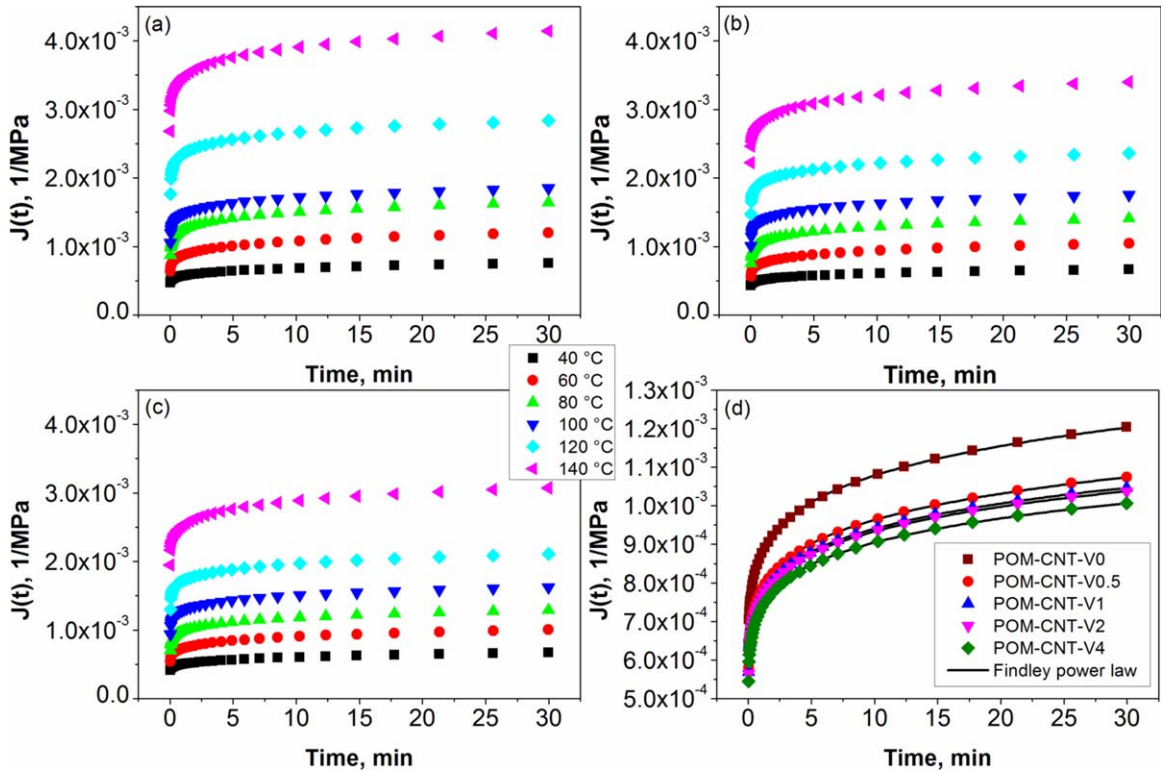

Figure 7. Creep compliance of various nanocomposites at different temperatures: (a) POM, (b) POM filled with 1 vol % CNT, (c) POM filled with 4 vol % CNT, and (d) the representative experimental curves and modeling results of different materials at 60°C. [Color figure can be viewed in the online issue, which is available at wileyonlinelibrary.com.]

nanotubes at each temperature which indicates an enhanced creep performance.

The time–temperature superposition principle (TTSP) is also a widely used method to predict the long-term creep performance from short-term creep behavior. The creep strain was measured at different temperatures between 40 and 140°C, respectively, under a constant load of 2 MPa for appropriate time scale. Master curves in form of creep compliance versus time were produced using TTSP, as is illustrated in Figure 8. Note that the master curve provides a useful prediction of the creep behavior over the time range up to 10^{11} min. It is visible that the nanocomposites present much better creep resistance in the studied time interval. The shift factor shows a good linear dependence on the temperature, as is shown in Figure 8.

Tribological Behaviors of Nanocomposites

Figure 9(a) shows the typical curves of the friction coefficients of pure POM and POM filler with 1 and 4 vol % carbon nanotubes as a function of sliding distance. As is shown, the friction coefficient arrives at a relatively stable value after a short running in period. Figure 9(b) shows the mean friction coefficients of different materials in the stable state of sliding. The incorporation of small amount of carbon nanotubes, for example, 0.5 and 1 vol %, results in increasing friction coefficient. However, the nanocomposites filled with 4 vol % present slightly lower friction coefficient than that of pure polymer matrix. The specific wear rate of the nanocomposites is shown in Figure 9(c). After incorporating carbon nanotubes, the wear resistance was impaired. Compared with pure polyoxymethylene, the addition

Table II. The Simulated Parameter of the Findley Power Law at 60 and 120°C

	60°C			120°C		
Materials	J_{F0} 10^{-4}%	J_{F1} 10^{-4} min^{-n}	n -	J_{F0} 10^{-4}%	J_{F1} 10^{-4} min^{-n}	n -
POM-CNT-V0	3.082	5.627	0.136	3.885	19.60	0.066
POM-CNT-V0.5	3.037	4.765	0.141	8.788	11.30	0.094
POM-CNT-V1	2.805	4.824	0.136	9.259	10.20	0.101
POM-CNT-V2	2.651	4.934	0.132	8.460	10.40	0.097
POM-CNT-V4	2.628	4.707	0.135	8.683	8.490	0.112

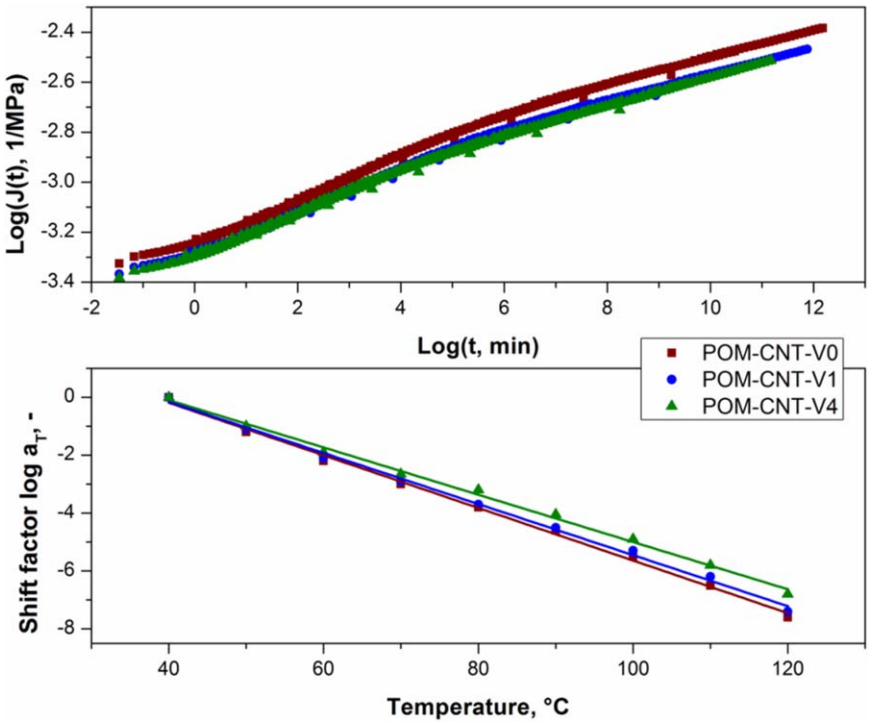

Figure 8. Master curves of different materials at a referent temperature of 40°C. [Color figure can be viewed in the online issue, which is available at wileyonlinelibrary.com.]

of 1 vol % carbon nanotubes leads to an increase in the wear rate by about 80%. It can be, therefore, concluded that for polyoxymethylene the carbon nanotubes has negative impact on the tribological properties without solid lubrication, although the mechanical properties and the creep resistance of the matrix were improved.

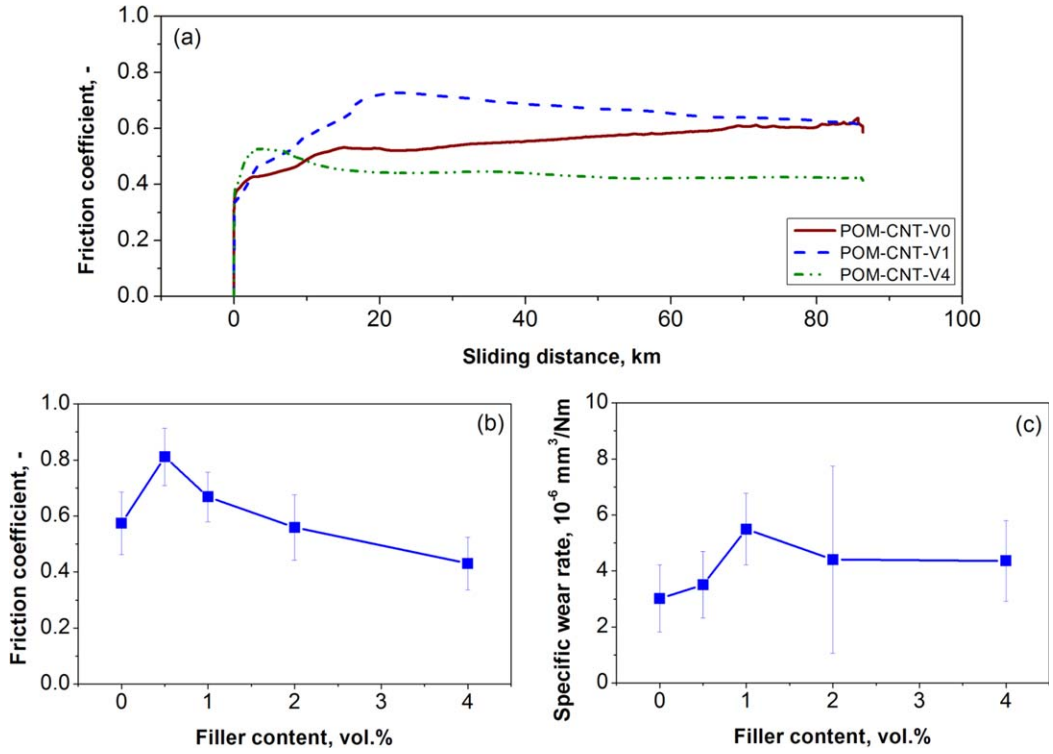

Figure 9. (a) Friction coefficient of nanocomposites as a function of sliding distance; (b) mean friction coefficients as a function of CNT content; and (c) specific wear rate of nanocomposites as a function of filler loading. [Color figure can be viewed in the online issue, which is available at wileyonlinelibrary.com.]

CONCLUSIONS

In this work, carbon nanotube reinforced polyoxymethylene was prepared using a masterbatch dilution process, to gain the best dispersion and distribution quality of CNT within POM matrix. The content of the carbon nanotube varied from 0 to 4 vol %. The dispersion and distribution quality of CNT within polyoxymethylene matrix are significantly improved using masterbatch dilution process. DSC measurements indicate very little change in the melting temperature and crystallinity of the nanocomposites relative to the matrix. The addition of CNT results in a significant enhancement in matrix stiffness and a marginal improvement in strength, accompanies with reduction in matrix ductility. By contrast, poor dispersion quality has no reinforcing effect in tensile strength. Similarly, the results of dynamical mechanical analyses show that the storage modulus of the nanocomposites increases with the filler content as expected with the 4 vol % showing the highest improvement compared to the matrix and better dispersion quality leads to higher storage modulus of the nanocomposites. The incorporation of carbon nanotube into polyoxymethylene has only minor influence on the α-transition temperature of virgin POM. The creep resistance of the polymer matrix is also pronounced improved after incorporating carbon nanotubes. However, the creep resistance among different nanocomposites, that is, 0.5, 1, 2, and 4 vol %, is not dramatically in the testing range which indicates that a quite low content of carbon nanotubes can effectively enhance the creep resistance of POM. The master curves that constructed using the time–temperature superposition principle showed the prediction of the long-term performance up to more than 10^{11} min in the time scale.

By addition of carbon nanotubes, the specific wear rate of POM is moderately increased and at low filler contents, the composite presents the highest wear rate and the highest friction coefficient as well. The mechanisms of the reduction of tribological property of POM after incorporation of carbon nanotube should be investigated in detail.

ACKNOWLEDGMENTS

The authors thank the German Research Foundation for the financial support according to the DFG-SCHL 280/19-1 and BASF SE, Ludwigshafen, Germany, for kindly supplying of the materials. They are also grateful to Mrs. C. Wagner, IFOS, Kaiserslautern and Mr. V. Demchuk, Polymer Engineering, Hamburg, for the helpful cooperation of the experiments.

REFERENCES

1. Iijima, S. *Nature* **1991**, *354*, 56.
2. Yang, J.-L.; Zhang, Z.; Schlarb, A. K.; Friedrich, K. *Polymer* **2006**, *47*, 2791.
3. Yang, J.-L.; Zhang, Z.; Schlarb, A. K.; Friedrich, K. *Polymer* **2006**, *47*, 6745.
4. Villmow, T.; Pegel, S.; Pötschke, P.; Wagenknecht, U. *Compos. Sci. Technol.* **2008**, *68*, 777.
5. Krause, B.; Pötschke, P.; Häussler, L. *Compos. Sci. Technol.* **2009**, *69*, 1505.
6. Thostenson, E. T.; Ziaee, S.; Chou, T. W. *Compos. Sci. Technol.* **2009**, *69*, 801.
7. Coleman, J. N.; Khan, U.; Blau, W. J.; Gun'ko, Y. K. *Carbon* **2006**, *44*, 1624.
8. Arranz-Andrés, J.; Blau, W. J. *Carbon* **2008**, *46*, 2067.
9. Zhao, X.-W.; Ye, L. *J. Polym. Sci. Part B: Polym. Phys.* **2010**, *48*, 905.
10. Yang, J.-L.; Zhang, Z.; Friedrich, K.; Schlarb, A. K. *Macromol. Rapid Commun.* **2007**, *28*, 955.
11. Sahoo, N. G.; Rana, S.; Cho, J. W.; Li, L.; Chan, S. H. *Prog. Polym. Sci.* **2010**, *35*, 837.
12. Müller, M. T.; Krause, B.; Kretzschmar, B.; Pötschke, P. *Compos. Sci. Technol.* **2011**, *71*, 1535.
13. Hosokawa, M.; Nogi, K.; Naito, M.; Yokoyama, T. In Nanoparticle Technology Handbook; Elsevier B. V.: Kidlington, **2007**.
14. Villmow, T.; Kretzschmar, B.; Pötschke, P. *Compos. Sci. Technol.* **2010**, *70*, 2045.
15. Sathyanarayana, S.; Hübner, C.; Diemert, J.; Pötschke, P.; Henning, F. *Compos. Sci. Technol.* **2013**, *84*, 78.
16. Li, Y.; Shimizu, H. *Polymer* **2007**, *48*, 2203.
17. Villmow, T.; Pötschke, P.; Pegel, S.; Häussler, L.; Kretzschmar, B. *Polymer* **2008**, *49*, 3500.
18. Zoo, Y. S.; An, J. W.; Lim, D. P.; Lim, D. S. *Tribol. Lett.* **2004**, *16*, 305.
19. Wang, C.; Dong, B.; Gao, G.-Y.; Xu, M.-W.; Li, H.-L. *Mater. Sci. Eng.* **2008**, *478*, 314.
20. Wacharawichanant, S.; Sangkhaphan, A.; Sa-Nguanwong, N.; Khamnonwat, V.; Thongyai, S.; Praserthdam, P. *J. Appl. Polym. Sci.* **2012**, *123*, 3217.
21. Sathyanarayana, S.; Wegrzyn, M.; Olowojoba, G.; Benedito, A.; Giménez, E.; Hübner, C.; Henning, F. *Express Polym. Lett.* **2013**, *7*, 621.
22. Pielichowska, K.; Dryzek, E.; Olejniczak, Z.; Pamula, E.; Pagacz, J. *Polym. Adv. Technol.* **2013**, *24*, 318.
23. Rong, M.-Z.; Zhang, M.-Q.; Zheng, Y.-X.; Zeng, H.-M.; Walter, R.; Friedrich, K. *Polymer* **2001**, *42*, 167.
24. Findley, W. N.; Lai, J. S.; Onaran, K. In Creep and Relaxation of Nonlinear Viscoelastic Materials: With an Introduction to Linear Viscoelasticity; Dover Publications, Inc.: New York, **1989**.